

## ELECTRONIC STRUCTURE AND PHOTOCHEMICAL REARRANGEMENTS OF MATRIX-ISOLATED $C_8H_{10}$ RADICAL CATIONS

T. BALLY, E. HASELBACH, S. NITSCHKE and K. ROTH  
Institut de Chimie Physique de l'Université, Pérolles, CH-1700 Fribourg, Switzerland

(Received in U.S.A. 7 October 1985)

**Abstract**—The  $C_8H_{10}$  isomers 1,3,5,7-octatetraene (OTE), 1,3,5-cyclooctatriene (COT) and bicyclo[4.2.0]octa-1,4-diene (BCO) were subjected to ionization by X-irradiation in argon matrices at 20 K. The electronic structure of the parent radical cations is discussed on the basis of their spectral properties and qualitative theoretical considerations. Photolysis of the cyclic cations leads to the formation of OTE<sup>+</sup> in at least six different conformation which can be distinguished by selective bleaching experiments. The complex band structure of the all-*trans*-OTE<sup>+</sup> absorptions is demonstrated to arise from the presence of this species in at least five different matrix sites. By very narrow-bandwidth irradiation, single sites can be bleached or populated and the resulting difference spectra allow a detailed vibronic analysis of all-*trans*-OTE<sup>+</sup>.

### INTRODUCTION

The spectra and structures of various polyene molecular cations in cryogenic matrices have recently begun to attract a great deal of interest.<sup>1-4</sup> In particular, the ring opening of cyclic to linear polyene cations and the photochemical interconversion of different "rotamers"<sup>†</sup> of the latter have come under close scrutiny.<sup>3,4,6</sup> In this paper, we wish to present extensions of our previous studies in this area<sup>1,3</sup> to the  $C_8H_{10}^+$  family of such compounds. For general discussions dealing with the subject of matrix-isolated open-shell organic cations ( $M^+$ ) and the techniques used to investigate them we refer to recent reviews.<sup>7</sup>

Before going into a discussion of our results we note that the group of Prof. Shida has independently conducted a very similar study on  $C_8H_{10}^+$  using Freon glass techniques.<sup>†</sup> Without forestalling the conclusions of their study we wish to point out that a comparison of theirs with the present findings demonstrates effectively the respective benefits and disadvantages of the two techniques: while Freon glasses prove superior for investigating metastable primary or intermediate  $M^+$ , the higher spectral resolution attainable in argon matrices generally allows a more detailed insight into the vibrational structure of those  $M^+$  that are amenable to observation in this medium. In order to fully exploit this advantage it often proves profitable to resort to very selective photolysis experiments, especially in cases like the present one where ionization initially results in a multitude of products.

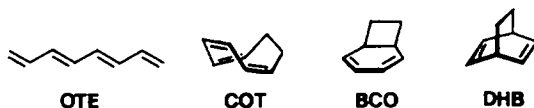
<sup>†</sup>In polyene cations, a clear distinction between single and double bonds can no longer be made. We have therefore proposed<sup>3</sup> to use the general term "rotamers" instead of conformers (pertaining to rotation around single bonds) or isomers (for double bond rotamers) to distinguish between different planar or periplanar linear polyene cations of a given composition. We will use the *E/Z* nomenclature to describe the geometry of individual polyene cation rotamers.

<sup>‡</sup>We would like to thank Prof. Shida for making his results available to us prior to publication.

<sup>§</sup>Presented in part by one of the authors of the present paper (T.B.) at the 1983 Gordon Conference on the "Spectroscopy of Matrix Isolated Species".

Such techniques were not available to Dunkin *et al.*, who have recently reported basic features of some  $C_8H_{10}^+$  in argon<sup>2</sup> without resolution of the multifaceted absorptions of the various involved linear polyene cations. We therefore found it valuable to present as a contribution to this symposium the results of our corresponding studies which have been going on for several years,<sup>§</sup> and may serve in addition to illustrate quite generally the techniques available in our laboratory.

The compounds used in the present study include 1,3,5-octatetraene (OT) and the cyclic precursors 1,3,5-cyclooctatriene (COT) and bicyclo[4.2.0]octa-2,4-diene (BCO). We will also mention bicyclo[2.2.2]octa-2,4-diene (dihydrobarrelene DHB) which was investigated in the abovementioned study.<sup>2</sup>



The techniques employed are described in detail under Experimental. Briefly, X-irradiation of a neutral precursor  $M$  embedded in an argon matrix doped with an electron scavenger serves to partially convert the former to the corresponding radical cation  $M^+$ . Since  $M^+$  usually absorb mainly in the visible, their electronic absorption (EA) spectra do not generally interfere with those of the precursors  $M$  and can be studied at leisure as long as cryogenic conditions are maintained. These spectra often contain complementary information to the photoelectron (PE) spectra of the neutrals and can serve to elucidate additional features of the ion's electronic structure.<sup>7</sup>

Often the parent  $M^+$  are, however, not observed, either because they are initially endowed with sufficient excess energy to surmount barriers for dissociation or rearrangement to more stable isomers, or because such barriers are low enough to be crossed with the available equilibrium thermal energy. A special case of the latter situation is found in the so-called "non-vertical cations"<sup>7</sup> which relax spontaneously to isomeric structures upon formation. Since hole trans-

fer from the (primary) solvent cations is more exothermic for argon ( $I_1 = 15.75$  eV) than for the Freons ( $I_{a,1} = 11-12$  eV) the incipient (secondary) substrate cations contain more excess energy if formed in an argon matrix. Furthermore, the lattice phonons of noble-gas matrices are notoriously poor acceptors of bond-stretching and bending vibrational quanta.<sup>10</sup> These two reasons may be responsible for the different extent of rearrangements observed upon ionization in Freon glasses vs argon matrices † In the case of X- or  $\gamma$ -irradiation, secondary photons from the radiochemical cascade may furthermore induce photo-rearrangements of M or M<sup>+</sup> as observed also in the present case.

Especially in the case of such molecular rearrangements upon ionization, the spectra may initially appear rather complex. However, they can often be successfully disentangled with the help of selective photolysis experiments which may furthermore yield rewarding insights into the interesting photochemistry of M<sup>+</sup>.<sup>7c</sup> This paper will show how far we can presently carry this methodology using standard equipment.

## RESULTS AND DISCUSSION

### Primary cations

Figure 1 shows the EA spectra of OTE, COT, and BCO, respectively, with a two-fold molar excess of CH<sub>2</sub>Cl<sub>2</sub> in a  $\sim 10^3$ -fold excess of argon after 2 h X-irradiation at 20 K (the spectrum prior to irradiation is already subtracted). Apart from the presence of a group of sharp peaks between 500 and 400 nm there is no similarity between the spectrum obtained from OTE and the other two which show in particular an intense broad band at  $\lambda_{max} = 360$  nm due to CH<sub>2</sub>Cl<sub>2</sub><sup>+</sup>.<sup>12</sup>

Apart from this we note a group of sharp peaks between 300 and 250 nm which are due to neutral OTE formed from the cyclic isomers in the process of X-irradiation (the top spectrum is cut off at 320 nm because from there on the spectrum is masked by absorptions of the neutral precursors). Comparison with the UV spectrum of authentic all-*trans* OTE in argon recorded at the same resolution (Fig. 1(d)) shows small but significant shifts between the individual peak maxima apart from a general broadening of all spectral features. We attribute this to the simultaneous formation of different conformers of OTE from COT and/or BCO which may furthermore occupy different sites in the argon matrix.

Note that the process of photochemical ring opening in an argon matrix is different for the two neutral cyclic isomers (Scheme 1).<sup>13</sup> While COT gives all-*trans* OTE (presumably in the all-*s-cis* conformation)<sup>14</sup> in a disrotatory electrocyclic reaction, BCO does *not*

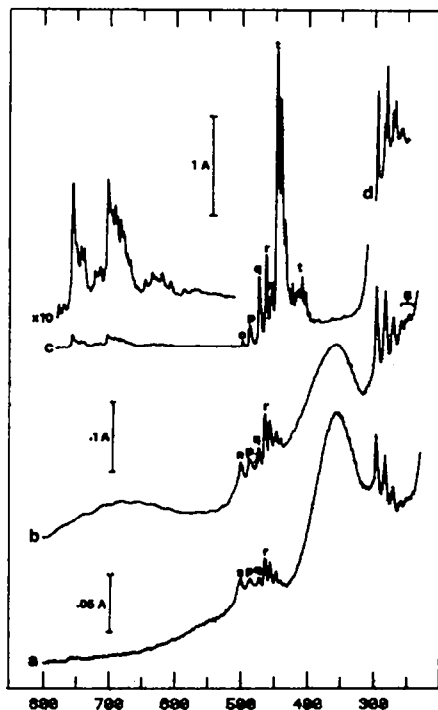
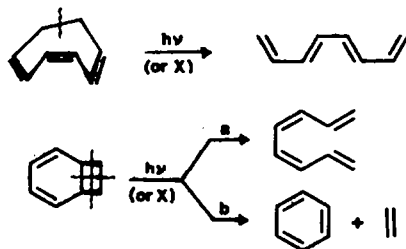


Fig. 1. Difference spectra obtained after 2 h X-irradiation of COT (a), BCO (b) and OTE (c) embedded in Ar at 20 K. Spectrum (d) shows the absorption of neutral OTE in Ar for comparison.

photoisomerize directly to COT because steric constraints impose a photochemically forbidden disrotatory pathway for this process. Instead, it prefers  $[2\pi + 2\pi]$ -cycloreversion to yield either *cis-cis*-OTE (path a) or benzene plus ethylene (path b) as primary photoproducts.<sup>13</sup> (In solution, the former product immediately recyclizes to COT, thus pretending a direct BCO  $\rightarrow$  COT photoisomerization.) In comparison to path a the second reaction is only a minor process under X-irradiation because the characteristic spectrum of benzene in argon shows up only very weakly (bands labelled B in Fig. 1(b)).

Next, we have to discuss the fate of the primary neutral species upon ionization. Unfortunately the strongest spectral features of BCO<sup>+</sup> are expected to occur in a region initially masked by CH<sub>2</sub>Cl<sub>2</sub><sup>+</sup> absorptions ‡ which makes it impossible to judge the amount of BCO<sup>+</sup> formed. However, the great similarity of the spectra obtained after X-irradiation of COT and BCO



Scheme 1. Photochemical reactions of COT and BCO in solid matrices.<sup>13</sup>

† Recent experiments on dicyclopentadiene radical cations carried out in both media illustrate effectively the notion that metastable primary or intermediate radical cations show up more clearly in Freon glasses.<sup>11</sup>

‡ We have also obtained the optical spectra of pure ionized BCO and COT in Freon glasses where the parent cations can be clearly distinguished. The results of this study and a discussion of the BCO<sup>+</sup> and COT<sup>+</sup> electronic structure and reactivity will be reported separately.<sup>15</sup>

Table 1. Thermochemical data for cyclic and open chain polyenes

Compound M	$\Delta H_f^\circ(M)$ [kcal mol <sup>-1</sup> ]	$I_{a,1}(M)$ [eV]	$\Delta H_f^\circ(M^+)$ [kcal mol <sup>-1</sup> ]
OTE	53.2 <sup>a</sup>	7.8 <sup>b</sup>	233.0
COT	46.3 <sup>c</sup>	7.9 <sup>d</sup>	228.5
BCO	46.4 <sup>e</sup>	8.0 <sup>f</sup>	230.5
DHB	32.5 <sup>g</sup>	8.5 <sup>h</sup>	228.5
Benzene + ethylene	19.8 <sup>i</sup>	9.24 <sup>j</sup>	245.4

<sup>a</sup> Calculated using the Benson group increment scheme<sup>16</sup> which is expected to give very reliable results for linear polyenes.

<sup>b</sup> Ref. 17.

<sup>c</sup> The enthalpies of hydrogenations published in Ref. 18 can be combined with the enthalpies of formation of the resulting saturated hydrocarbons<sup>19</sup> to give the enthalpies of formation of the listed compounds.

<sup>d</sup> Ref. 20.

<sup>e</sup> From the enthalpy of isomerization to COT.<sup>21</sup> The resulting figure matches quite well with that obtained from the enthalpy of hydrogenation of BCO<sup>22</sup> which together with the enthalpy of formation of bicyclo[4.2.0]octane<sup>19</sup> give  $\Delta H_f^\circ$  (BCO) = 45.2 kcal mol<sup>-1</sup>.

<sup>f</sup> Prof. Gleiter has kindly provided us with a copy of the original spectrum to allow a precise determination of the first PE band onset.<sup>23</sup>

<sup>g</sup> Ref. 24. See also footnote c above.

<sup>h</sup> Ref. 25.

<sup>i</sup> Ref. 19. Note that this figure does not include the formation of a (benzene·ethylene)<sup>+</sup> complex from the isolated fragments which amounts to approx. 10 kcal/mol.<sup>15</sup>

<sup>j</sup> Ref. 26.

<sup>k</sup> Ref. 27.

suggests extensive rearrangement of BCO upon ionization. Since there is virtually no driving force for a thermal BCO<sup>+</sup> → COT<sup>+</sup> isomerization (Table 1), we conclude that it must involve ionic excited states which may be populated in the highly exothermic hole transfer from Ar<sup>+</sup>. It can actually be shown with orbital correlation diagrams that rearrangement to COT<sup>+</sup> should occur readily from the D<sub>1</sub> state of BCO<sup>+</sup> (and *vice versa*).<sup>†</sup> All -E-OTE<sup>+</sup>, considered to be the major product in the experiment with all-*trans*-OTE, is formed only in minor amounts from COT and BCO. Concerning the photoproducts of BCO (Scheme 1) we note that cyclization processes are generally not observed in solid matrices and hence ionized *cis-cis*-OTE is unlikely to contribute to the signals of COT<sup>+</sup>. Furthermore, benzene<sup>+</sup> and ethylene<sup>+</sup> do not absorb strongly in the spectral region investigated and would therefore escape detection. Finally, the broad hump between 800 and 500 nm in Fig. 1(b) proved to be insensitive to photolysis and annealing and may therefore be due to a neutral radical or closed-shell ionic byproduct.<sup>‡</sup>

It is interesting to compare our initial spectra to those obtained by Dunkin *et al.* in their argon-resonance ionization experiments.<sup>2</sup> We note in particular that the spectral features attributed to the primary cations, i.e. the 500 nm band in the case of COT and the group of peaks starting at 448 nm in the case of OTE (assignments see below) are more prominent in our argon matrix and even dominant in the Freon

glass experiments.<sup>1</sup> This is probably due to the fact that ionization occurs *prior* to matrix isolation in the argon-resonance experiments. This allows extensive rearrangements to occur before definitive trapping of the ions while such reactions face matrix-imposed barriers under our conditions. The difference between the argon matrix and the Freon glass experiments<sup>1</sup> can in turn be explained by invoking the arguments outlined in the final part of the Introduction.

#### Selective photochemistry

In order to analyze the group of bands between 500 and 400 nm and the weak spectral features between 800 and 600 nm we took recourse to the technique of selective narrow-band photolyses which had previously led the Kyoto group<sup>6</sup> and us<sup>3</sup> to a successful identification of all species occurring upon ionization of cyclohexadiene or hexatriene.

Of course the present problem is considerably more complex in that we already set out with two different cyclic isomers (and many more can be envisaged although they are unlikely to be involved). At the open-chain polyene level we are faced with *five* instead of three internal bonds, each of which can locally define an *E*- or a *Z*-conformation, giving a total of 20 distinguishable "rotamers"<sup>28</sup> instead of the six we had to deal with in the hexatriene case. Furthermore, many of these 20 rotamers will have to adapt non-planar geometries and the complexity of the site structure will also increase with increasing chain length. Due to these factors we could not hope to completely disentangle the system and therefore tried to obtain the maximum information within the limitations of our experimental conditions.

*Long-wavelength photolyses.* In a first set of experiments we tried to find the minimum energy required to induce photochemical rearrangements. Since

<sup>†</sup>For general discussion of the principles governing rearrangements of open-shell species see Ref. 29.

<sup>‡</sup>Note added in proof: Recent experiments<sup>27</sup> seem to indicate that this absorption is due to a (benzene·ethylene)<sup>+</sup> complex.

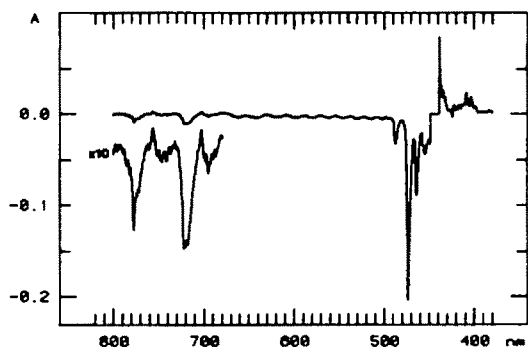


Fig. 2. Difference spectrum obtained after 3 h irradiation of a sample of ionized OTE at 772 nm. Between 450 and 440 nm no spectral information is available because  $A \geq 3.0$  in the component spectra.

initially all absorptions above 500 nm were either very weak or even intangible by our methods, only photolyses at wavelengths where the argon plasma arc shows strong emission lines were considered. Thus, beginning at 811 nm sluggish but measurable bleaching of band *n* in Fig. 1 ( $\lambda_{\max} = 502.0$  nm) could be induced which was accompanied by an increase in the 490–440 nm group of peaks. This proves that the species absorbing at 502 nm has a lower-lying excited state as it is expected for  $COT^+$ . Upon irradiation at the 772 nm emission line, new changes began to occur. These are documented in Fig. 2, which shows the results of an experiment with ionized  $OTE^+$  where the cations absorbing at this wavelength are initially present in higher concentration thus giving better difference spectra. In fact it is mainly the species labelled *q* in Fig. 1 which is bleached in this process with concomitant formation of *t* (observed mostly in the difference spectrum due to its overly intense absorption). Irradiation at  $\lambda < 772$  nm resulted in more complex spectral changes but the general sluggishness of the associated processes made it difficult to use such long-wavelength irradiations for diagnostic purposes as in the previous case of hexatriene.<sup>3</sup> Nevertheless, the above results argue against the conclusion of the Virginia group that "irradiation (...) in the red absorption system does not provide sufficient internal energy to promote rearrangement(s)."<sup>2</sup>

**Photochemical transformations of  $COT^+$ .** Peak *n* assigned to  $COT^+$ <sup>15</sup> can also be bleached by irradiation at 500 nm with concomitant formation of the 490–440 nm peaks, but interestingly a different behaviour is observed when narrow-band photolysis at 505 nm is applied (Fig. 3): under these conditions, a new species with a broad absorption maximum at  $\sim 560$  nm accumulates apart from the 490–440 nm group of peaks. Subsequent irradiation at 560 nm forms a species with  $\lambda_{\max} = 500.2$  nm which does *not* however, revert measurably to the former species upon renewed photolysis at 505 nm.

Regarding the assignment of the 560 nm transient we note that the  $\pi$ -system of  $COT$  is expected to undergo planarization upon ionization due to an increase in  $\pi$ -bond orders across the essential single bonds (a prediction which is well borne out by MNDO calculations<sup>15</sup>). Since the ethano bridge will be twisted to

relieve angular strain, the equilibrium geometry of  $COT^+$  appears well disposed for ring opening to a *helical* conformer of all-*Z*- $OTE^+$ . A frontier orbital diagram (Scheme 2) shows that the ground states of  $COT^+$  and  $OTE^+$  do not correlate for this reaction because they are of opposite symmetry with respect to the twofold symmetry axis shared by both species, and therefore a ground-state adiabatic process is *state-symmetry* forbidden. However, the ground configuration of  $OTE^+$  correlates with either of the two first excited configurations (HOMO  $\rightarrow$  LUMO or HOMO-1  $\rightarrow$  HOMO) which constitute the first two excited states of  $COT^+$ . Hence the  $OTE^+ \rightleftharpoons COT^+$  interconversion can occur adiabatically only upon electronic excitation.

Actually, the unique Moebius-type disposition of  $\pi$ -orbitals which occurs only in this special conformation of  $OTE^+$  may explain the difference in spectral appearance of this species compared to the other observed rotamers (see Scheme 2): introduction of an antarafacial bonding interaction between the termini (or the terminal double bonds) of an  $OTE$   $\pi$ -framework results in a *raising* of  $\pi_3$  and a lowering of  $\pi_4$  leading to a pronounced lowering of the  $\pi_3 \rightarrow \pi_4$  excited configuration. How the LUMO is affected depends on the extent of overlap between the termini (if 1–8 interaction predominates, it is raised, if 1–7 and 2–8 interactions predominate, it is lowered). In any event, interaction between the  $\pi_3 \rightarrow \pi_4$  and the  $\pi_4 \rightarrow \pi_3$  excited configurations of the same symmetry<sup>1</sup> is strongly attenuated due to their increased energy separation which may lead to a lowering of energy of the second excited state as well. Similar qualitative considerations lead also to a rationale for the observed broad band shape which hints at pronounced geometrical changes in the course of excitation:  $\pi_4 \rightarrow \pi_3$  electron promotion leads from a bonding to an antibonding FMO contribution to the 1–8 interaction which may well result in strong geometrical changes of a type not suffered by the other rotamers which all show comparatively sharp EA bands.

Although such a helical  $OTE^+$  geometry seems ideally suited for recyclization to  $COT^+$ , the observed irreversibility of the above photochemical transformation together with the small but significant changes in  $\lambda_{\max}$  and band shapes indicates that this process does in fact not occur. Instead, all-*z*- $OTE^+$

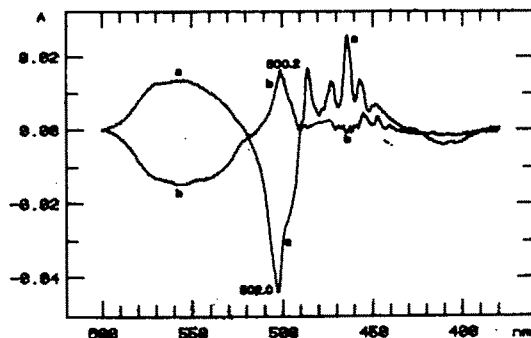
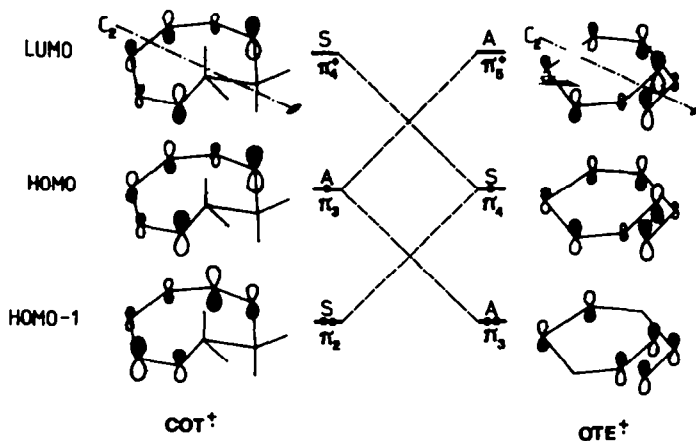


Fig. 3. Difference spectra obtained after photolysis of ionized  $COT$  (or  $BCO$ ) at 505 nm (a) and subsequently at 560 nm (b).



Scheme 2. Frontier orbital correlations for  $COT^+ \rightarrow OTE^+$  ring opening. (The drawing of the  $COT^+$  geometry is in accord with the MNDO calculated equilibrium geometry.<sup>15</sup>)

probably undergoes rotation around one of the central bonds to yield some other  $OTE^+$  rotamer which now has a "normal" linear array of  $\pi$ -orbitals and hence a similar spectral appearance as all other such species. Indeed, a small band with  $\lambda_{max} = 500$  nm is also observed after ionization of all-*trans*- $OTE$  (see Fig. 1(c)), thus lending support to the above tentative conjecture.

**Transformations among  $OTE^+$  rotamers.** Next, the selective bleaching of bands o through s between 500 and 455 nm was investigated. The results of this procedure are summarized in Fig. 4 which shows on the one hand the evolution of the band structure between

500 and 455 nm and on the other hand the differences obtained by subtracting the spectra obtained before and after photolysis at the wavelength indicated by the open triangle. It can be seen that bands o through s can be consecutively bleached although not always completely because of the establishment of photostationary equilibria among the different species involved (see in particular e  $\rightarrow$  f). The expanded insets show the respective concomitant spectral changes between 800 and 600 nm which allow in some cases the identification of the first EA bands of the species whose main absorption lies at the wavelength of irradiation. The analysis of these weak red bands (col-

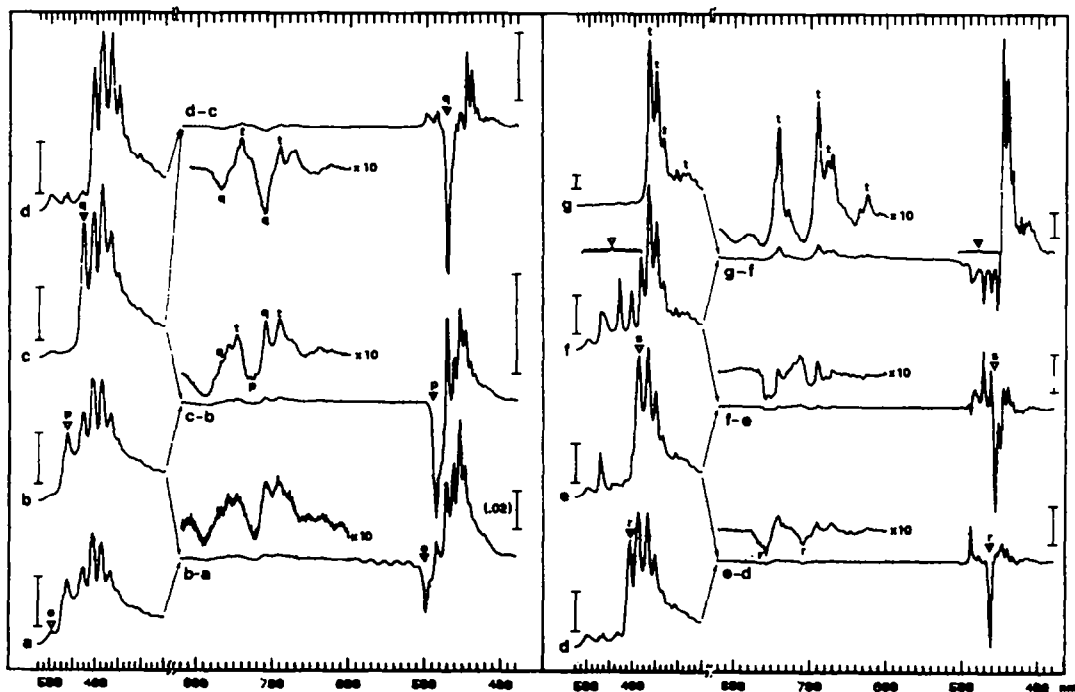


Fig. 4. Results of selective bleaching experiments. Sequence of events is from bottom to top, first on the left then on the right-hand side of the figure. Letters o through t follow the nomenclature previously used<sup>2</sup> and designate individual  $OTE^+$  rotamers. The vertical bars represent 0.2 Å except in difference spectrum b-a.

lectively labelled "y" in Ref. 2) is made rather difficult by the fact that groups of molecules occupying different sites in the argon matrix turn out to show considerable shifts in their 800–600 nm peak maxima (much less than in their 500–400 nm peaks). Since in the experiments summarized in Fig. 4, all sites were bleached in each step, broad bands often resulted in the red spectral region.

In the last step ( $f \rightarrow g$ ) all bands between 500 and 455 nm were bleached collectively by moving back and forth between the different absorptions in this range until they had all disappeared. What remains is species t, responsible for the main absorption after ionization of all-*trans*-OTE and hence assigned to the corresponding parent cation. Great care has to be taken to exclude light at  $\lambda \leq 450$  nm from the sample giving spectrum g because it was found that exposure of the unshrouded cryostat to diffuse ambient light led to the rapid establishment of a new photostationary equilibrium involving all species o through t. However, renewed exhaustive photolysis between 500 and 450 nm quantitatively reforms the t-absorptions, indicating complete reversibility of these photo-rearrangements.

With regard to the assignment of bands o through s we note that the observation of only six species apart from all-*trans*-OTE<sup>+</sup> (counting also the helical all-*cis* rotamer formed as a primary product of COT<sup>+</sup> photolysis, see Scheme 2) is actually quite amazing in view of the theoretical complexity of the system.<sup>28</sup> Apparently, only a few of the 20 possible OTE<sup>+</sup> rotamers have a spectroscopically traceable existence in solid argon but unfortunately the present results do not allow an unambiguous identification of these particular species. From above, we note that the one responsible for band o is most probably formed by single bond rotation from the helical all-*cis* rotamer (the primary product of COT<sup>+</sup> ring opening) and the rather selective q  $\rightarrow$  t photoisomerization (see d-c in Fig. 4) suggests that the same relationship holds also for all-*trans*-OTE<sup>+</sup> and the rotamer with the q-absorption. Furthermore, our earlier experience with hexatriene<sup>+</sup> suggests for the present case that the main OTE<sup>+</sup> absorption should suffer a red shift in relation to the number of local *cis* configurations found in a given rotamer. The site-selective photolysis experiments to be described separately<sup>28</sup> will yield some more detailed insight into this matter.

#### The spectrum of all-*trans*-OTE<sup>+</sup>

**Theoretical aspects.** The EA spectra of polyene cations in general and OTE<sup>+</sup> in particular have recently been analyzed in a comprehensive fashion.<sup>1</sup> According to this analysis (which was unfortunately not considered in the recent discussion of the OTE<sup>+</sup> spectrum<sup>2</sup>) a single-configuration picture as it is commonly and successfully employed in the interpretation of polyene PE spectra is ill-suited to rationalize the EA spectra of the corresponding molecular ions. In particular, such a model predicts the transition moments for  $\pi_{n-1} \rightarrow \pi_n$  and  $\pi_n \rightarrow \pi_{n+1}$  ( $n = \text{HOMO}$ ) electron promotion to be nearly equal, in obvious contradiction to the observation of a weak red and an intense blue band in all polyene<sup>+</sup>.<sup>1</sup> However, allowance for configuration interaction (CI) between the two target excited configurations ( $\pi_{n-1}^1 \pi_n^2$  and

$\pi_n^2 \pi_{n+1}^1$ ) which are close in energy and of the same symmetry opens the way to a simple explanation of this important phenomenon: while the two transition moments add up in the (higher energy) positive CI combination, they nearly cancel in the negative one.<sup>3b</sup> This effect becomes more pronounced as the chain length increases, in accord with experimental observations. Therefore a description of polyene<sup>+</sup> excited states in terms of "simple hole promotions" becomes increasingly inadequate for longer chains.

**Analysis of the red band system.** Figure 5 shows a wavenumber plot of the first and second band systems of all-*trans*-OTE<sup>+</sup> as obtained from ionized COT (a) or OTE (b) after exhaustive photolysis between 500 and 450 nm (ionized BCO gives roughly the same spectrum as COT). While the blue bands are very similar in appearance (apart from a very small general shift) there are pronounced differences in the appearance of the red band system: its fine structure is very complex and sharp when the precursor is all-*trans*-OTE but comparatively simple and broad if originating from COT or BCO. Interestingly, important changes in the fine structure of both bands occur upon annealing of the sample giving spectrum (b) to a temperature where evaporation of argon begins while spectrum (a) remains virtually unchanged under the same conditions. Figure 5(c) shows the result of such an experiment for the former case (after recooling to 20 K to avoid complete evaporation of the matrix).

We believe that the observed transformations are due to changes in the relative population of different matrix sites by all-*trans*-OTE<sup>+</sup>. Using the relatively simple spectrum (a) and the very similar difference spectra (g)–(f) in Fig. 4 as a lead, we discerned four types of vibrational intervals (approximately 220, 330, 1010, and 1420 cm<sup>-1</sup>) in the red bands, as depicted at the bottom of Fig. 5. Application of the scales thus obtained to the more complicated spectra (b) and (c) revealed the presence of five spectroscopically distinguishable sites. Assuming that all of these sites show an identical set of vibrational progressions permitted every single peak in the red band systems of spectra (b) and (c) to be assigned to one of the five sites A–E while allowing at the same time for a more precise determination of the vibrational intervals (top of Fig. 5). Table 2(a) lists the results of this analysis along with the exact absolute values as obtained with a peak search algorithm. It shows that the vibrational intervals are in fact not identical for the different sites. Since the red band systems were recorded at 0.2 nm spectral and digital resolution (ten data points per nm), the observed variations, especially in the  $\sim 1010$  cm<sup>-1</sup> progression, are significant and real.

**Site-selective bleaching experiments.** In spite of the sharp absorptions which separate out on annealing (Fig. 5(c)), a vibrational analysis of the blue band system turned out to be more difficult. After various combinations of annealing and photolysis experiments using our conventional optical setup (allowing down to 2.5 nm fwhm irradiations) proved unfruitful for the complete unravelling of this band structure, recourse was taken to a technique which permitted site-selective isomerizations to be studied. For this purpose, photolyses were carried out through the double monochromator of our spectrophotometer (Experimental), whereby reasonably efficient bleaching could be effected down to 0.25 nm fwhm. An

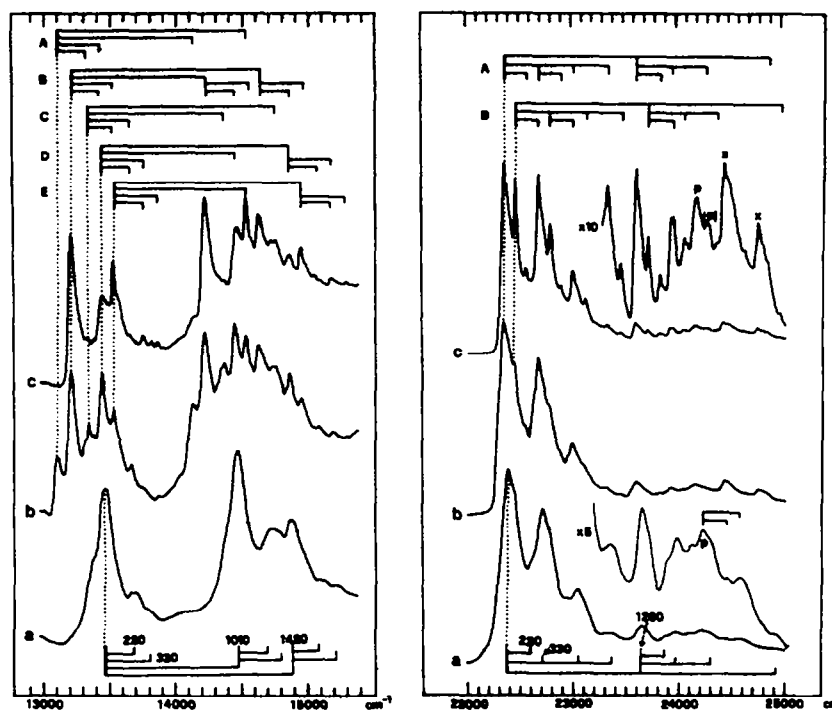


Fig. 5. First and second band system of *all-trans*-OTE<sup>+</sup> obtained from ionized COT (a) or OTE (b) after bleaching of all other species; (c) sample giving spectrum (b) annealed and refrozen (see text). Average numbers for vibrational intervals indicated on the bottom, for details see Table 2. A–E and X are different sites.

Table 2(a). Peak positions and assignments for *all-trans*-OTE<sup>+</sup>: red band system<sup>a</sup>

Peak pos. [nm] Spectrum b	Vibrational intervals in different sites (cm <sup>-1</sup> ) <sup>b</sup>					Peak pos. [nm] Spectrum a
	A	B	C	D	E	
762.6	origin	origin				
756.9 [757.1]						
749.3			origin			
743.0				origin		742.9
738.7 [739.2]					origin	
731.5				227		730.3
727.1					225	724.2
721.0					342	
707.3	1025					
702.9		1015 [1019]				
695.6			1030			
692.0		+224		1007		690.8
[691.4]		[+236]		[1017]		
688.0	1422				1007 [998]	
[686.3, sh]		+340				
683.5		1419 [1423]				
677.7			1412		+221	678.5
672.6		+234 [+237]		1421		672.1
668.6					1420 [1422]	
[668.9]						
662.7			+330	+223		
658.2				+333	[+234]	
[653.8]					[+345]	

<sup>a</sup> Compare Fig. 4, left-hand side.

<sup>b</sup> To  $\pm 2$  cm<sup>-1</sup>. Numbers in square brackets are taken from spectrum c, the others are either identical in spectra b and c or occur only in spectrum b (the last two columns belong to spectrum a). Numbers with a plus sign represent combinations based on the last fundamental immediately above in the same column.

Table 2(b). Peak positions and assignments for all-*trans*-OTE<sup>+</sup>: blue band system<sup>a</sup>

Peak pos. [nm] Spectrum c	Intervals in different sites [cm <sup>-1</sup> ] <sup>b</sup>			Peak pos. [nm] Spectrum c
	A	B	X	
447.8	origin		origin	446.6
445.6		origin		
443.5	(215) <sup>c</sup>			
441.3	330	(218) <sup>c</sup>	330	440.1
439.0		337		
437.1	+220			
434.9	2 × 330		2 × 330	433.8
432.6		2 × 337		
428.7	3 × 330		3 × 330	428.1
426.4		3 × 337		
423.9	1260		1265	422.7
421.8		1266		
419.8	+230			
418.0	+330		+230	418.6
417.6		+240	+330	417.0
415.8		+337		
413.9	1830 <sup>d</sup>		2 × 230	414.5
411.9		1836 <sup>d</sup>	1836 <sup>d</sup>	412.8
409.5	impurity		+230	409.0
404.5	impurity		+340	407.0

<sup>a</sup> Compare Fig. 4, right-hand side.

<sup>b</sup> To  $\pm 5$  cm<sup>-1</sup>. See also caption for Table 2(a).

<sup>c</sup> Assignment uncertain. May also be origin of another site.

<sup>d</sup> Probably origin of next electronic transition (see text).

account of the full set of investigations carried out in this fashion goes beyond the scope of this article and is presented elsewhere.<sup>28</sup> However, the results of one particular such experiment need mentioning because it yielded a breakthrough in the resolution of the present question: starting with the spectrum in Fig.

4(c), 110 min of 0.3 nm fwhm irradiation at 476 nm (the onset of peak q) gave the difference spectrum shown in Fig. 6. The remarkably well-resolved fine structure (fwhm of the t-absorptions about 70 cm<sup>-1</sup>) permitted a full vibrational analysis of both q (peaks pointing down) and t (peaks pointing up). The 230,

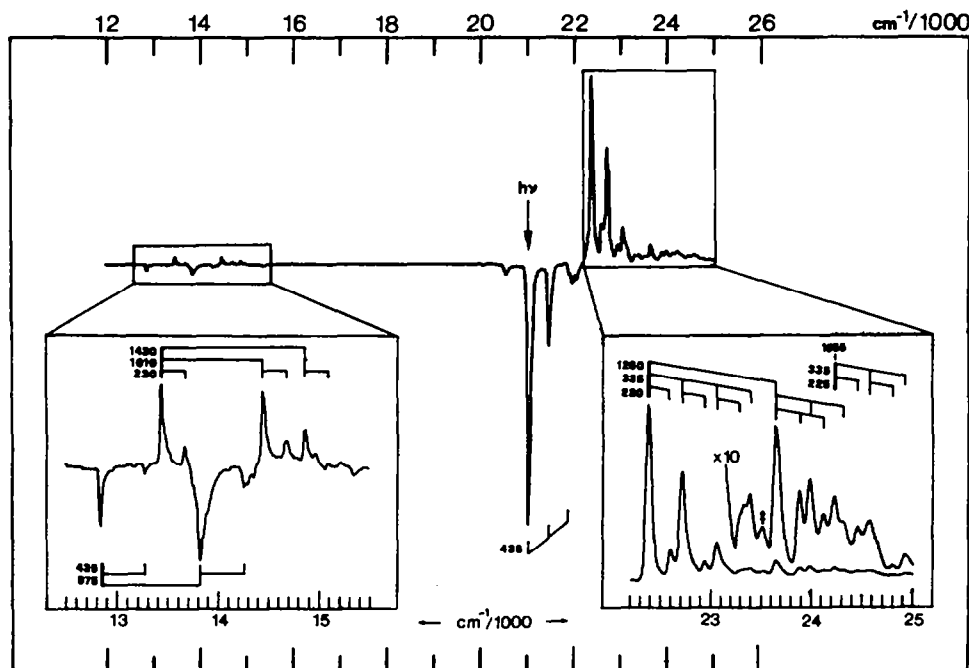


Fig. 6. Results of 0.3 nm fwhm irradiation of a sample showing strong q-absorptions at 475.9 nm (21,013 cm<sup>-1</sup>). The expanded insets show high-resolution scans (0.2 nm spectral slitwidth, 0.1 nm digital resolution) of the boxed regions together with a vibrational assignment (see text).



110 and  $1430\text{ cm}^{-1}$  progressions (and combinations thereof) from Fig. 5 showed up again in the red band system, thus confirming our above analysis (the  $330\text{ cm}^{-1}$  progression is hidden in the main red  $q$  peak) and two progressions of  $435$  and  $975\text{ cm}^{-1}$  were found for the two excited states of  $q$ . Furthermore, the spectrum confirms the clean  $q \rightarrow t$  interconversion suggested already by Fig. 4(d-c).

**Analysis of the blue band system.** Most importantly, the right expanded inset of Fig. 6 presents the blue band system of a single site of  $t$  (actually site D, judged from the position of the red band onset) together with an assignment of every single peak (except the one at  $23,510\text{ cm}^{-1}$  marked with a question mark) in terms of three vibrational progressions, i.e.  $220$ ,  $335$  and  $1260\text{ cm}^{-1}$  and combinations thereof. Separately drawn is a progression starting at  $1855\text{ cm}^{-1}$  from the 0-0 transition with its attached  $225$  and  $335\text{ cm}^{-1}$  members. Now the highest energy framework vibration of all-*trans*-OTE lies at  $1608\text{ cm}^{-1}$ ,<sup>30</sup> a value which remains virtually unchanged after ionization ( $\nu_{C=C} = 1610\text{ cm}^{-1}$ ).<sup>17</sup> On the other hand it increases upon excitation of OTE to the  $1^1B_u$  ( $\nu_{C=C} \sim 1640\text{ cm}^{-1}$ )<sup>31</sup> or, more pronouncedly, to the  $2^1A_g$  state ( $\nu_{C=C} = 1755\text{ cm}^{-1}$ ),<sup>32</sup> in contrast to what one expects from the changes in  $\pi$ -bond orders.<sup>33</sup> Although we could detect no vibrational progression in this frequency range,<sup>†</sup> we hesitate to assign the peak at  $1855\text{ cm}^{-1}$  above the  $2^2A_u$  band origin to a  $C=C$  vibrational progression because this would imply a  $\sim 245\text{ cm}^{-1}$  change from the corresponding ground-state frequency,<sup>17</sup> more than can be reasonably expected. Since this peak occurred reproducibly in all experiments, irrespective of the  $C_8H_{10}$  precursor and changed its intensity in concert with the other  $t$  absorptions upon photolysis, it must, however, belong to this species. We therefore propose that it represents the origin of the third electronic transition of OTE $^+$ . Indeed, open-shell PPP-CI calculations<sup>1</sup> predict a symmetry-forbidden ( ${}^2B_u \leftarrow {}^2B_u$ ) transition  $0.21\text{ eV}$  ( $= 1700\text{ cm}^{-1}$ ) above the strong  ${}^2A_u \leftarrow {}^2B_u$  excitation. This transition may well gain some intensity in a rigid matrix where the molecule is likely to be distorted from  $C_{2h}$  symmetry.

Carrying over these new insights to the spectra on the right-hand side of Fig. 5, all peaks can now be assigned with the exception of those marked with a  $\times$  which represents an impurity which always accompanies ionized OTE (but not OTE $^+$  formed from the cyclic precursors). These latter absorptions are insensitive to photolysis and annealing and therefore belong to a non-ionic by-product of OTE X-irradiation.

With regard to the previous vibrational analysis<sup>2</sup> we note that it failed to account for the site-structure discussed above. Since by accident some of the site shifts in the red band system match with true vibrational progressions, it led serendipitously to correct numbers in some cases whereas other intervals proposed in Ref. 2 are not supported by the present

data (notably the  $C=C$  stretching vibrational progression observed previously in emission).<sup>17</sup>

Finally, we note that annealing apparently results mainly in changes in the site *populations* but not the site *structure* in that the peak positions undergo only very small shifts upon annealing and subsequent refreezing. The site structure therefore seems to be an inherent property of the matrix which can host OTE $^+$  only in a limited number of different predefined cavities. These cavities appear to impose rather important geometry changes on this cation as judged from the size of the observed EA spectral shifts ( $430\text{ cm}^{-1}$  between the two most "distant" sites) as well as the change in vibrational structure (up to  $30\text{ cm}^{-1}$  in the  $1010\text{ cm}^{-1}$  progression).

## CONCLUSIONS

Concerning viewpoints of methodology, the present work offers several contributions to this symposium on radical ions. We first note that the initial composition of species after impact of ionizing radiation on neutral precursors  $M$  depends strongly on the surrounding medium. Freon glasses<sup>3</sup> prove superior in stabilizing metastable primary or intermediate  $M^+$  while the presently employed argon matrices, doped with an electron scavenger, often yield several products derived from  $M$  or  $M^+$  by rearrangements. Even more complex are the initial results if gas phase ionization (e.g. by charge resonance or photoionization)<sup>2</sup> precedes trapping of the ions in the matrix. Two factors are mainly responsible for this medium dependency.

(1) The excess energy deposited in the incipient ions after hole transfer increases from a freon to an argon matrix and, presumably, to charge exchange with (or photoionization by) argon in the gas phase.

(2) The efficiency for quenching of the excess energy decreases in the same order.

The multitude of initial products in the argon matrix, yielding a complex spectral pattern, requires selective narrow-bandwidth photolysis experiments which interconvert or bleach existing species or form new ones. A distinction between radical cations and neutral or closed-shell ionic species can be achieved in the same way since the latter usually prove less sensitive to such treatments.

The higher spectral resolution attainable in noble gas matrices facilitates the analysis of spectra provided adequate equipment is available, e.g. highly monochromatic light sources, sensitive spectrometers and digital data workup to yield difference spectra. Besides this analytical aspect such experiments often yield an interesting insight into the photochemistry of such ions.

Assignment of the various ionic species and mechanistic discussion of their interconversions are generally based on information about their electronic structure gained from photoelectron spectroscopy of  $M$  as well as on theoretical calculations. However, it must be noted that no theoretical model of practical use is currently available which allows a reliable prediction of the spectral shifts and variations in absorptivity of different polyene $^+$  rotamers. Symmetry arguments can be employed to explain some of the observed features and to distinguish between ground-

<sup>†</sup>One could argue whether the observed progression at  $1260+335 = 1595\text{ cm}^{-1}$  is due to the sought  $C=C$  stretching vibration. The observed *increase* of this frequency upon excitation of neutral OTE<sup>31,32</sup> would, however, speak against such an assignment.

and excited-state processes. Further evidence is accumulated that polyene<sup>+</sup> spectra require a discussion in terms of two *mixed* configurations of "Koopmans'" and "Non-Koopmans'" type, respectively.

The high spectral resolution discussed above led to the finding that in the specific case of pure all-*trans*-OTE<sup>+</sup> the absorptions are composed of five distinguishable sets of spectra which differ mainly in their absolute band positions and to a lesser degree in their vibrational intervals. This becomes evident upon controlled annealing of the sample which results in changes within the complex band pattern indicative of a change in *population* of different sites within the argon matrix. However, the absolute band positions remain unchanged in this process which leads to the conclusion that the site's *structure* is an intrinsic property of the argon matrix which can host a given solute ion only in a limited number of predefined cage structures. Since electronic interactions between argon and OTE<sup>+</sup> are small, the observed spectral shifts for different sites and the small variations in vibrational structure may be rationalized by invoking differential deviations from planarity of the  $\pi$ -system.

Finally, site-selective isomerizations<sup>28</sup> can be induced by decreasing the irradiation bandwidth to  $\leq 0.5$  nm fwhm. The corresponding well-resolved and uncongested difference spectra allow a detailed vibrational analysis of the involved species.

## EXPERIMENTAL

**Materials.** Octatetraene was synthesized according to Gavin *et al.*<sup>34</sup> with the modifications described in Ref. 1. 1,3,5-Cyclooctatriene was purchased from Organometallics and was purified by preparative GC on ODP. Bicyclo [4.2.0]octa-2,4-diene was similarly separated from the former commercial product whereby the temperature of the injection block was, however, held at 180° to ensure full equilibrium between the two isomers. Argon was of 99.995% purity and CH<sub>2</sub>Cl<sub>2</sub> which was used as an electron scavenger was analytical grade.

**Sample preparation and apparatus.**<sup>35</sup> 1:2 mixtures of the hydrocarbons and CH<sub>2</sub>Cl<sub>2</sub> diluted with a 1000–2000 molar excess were prepared on a special vacuum line with the help of absolute pressure transducers (Validyne AP10/DM256). The mixture was then deposited at a rate of  $\sim 1$  mmol h<sup>-1</sup> onto a sapphire window mounted on the tip of a closed-cycle duplex-type cryostat (Air-Products CSW 202) held at  $\sim 20$  K. Ionization was effected by 2 h X-irradiation through a beryllium window. Optical spectra were recorded on a Perkin-Elmer Lambda 9 UV/VIS/NIR spectrophotometer interfaced to a PE 3600 microcomputer which was in turn connected to a PDP 11/34 minicomputer where the spectra were worked up digitally. Full spectra were usually recorded with a spectral slitwidth of 0.4 nm and five data points per nm. For vibrational analyses, partial spectra taken at twice the above resolution were used.

**Photolyses.** All experiments except the last one shown in Fig. 6 were carried out by focusing the light of an argon plasma arc run at 1 kW into a *f*-3.4 monochromator with a grating blazed at 500 nm. Slits were usually set at 1 mm corresponding to a spectral fwhm of  $\sim 4.5$  nm and reduced to half this value in certain cases. Because of the extraordinary photosensitivity shown especially by OTE<sup>+</sup> great care was taken to shield the sample from ambient light so the unperturbed effects of selective irradiation could be studied. Site-selective bleaching was effected by focusing the argon plasma light into the optical system of the Lambda 9 spectrophotometer which was set at 0.25–0.5 nm spectral reso-

lution. During these experiments the sample had to remain carefully fixed within the compartment of the instrument to assure that measurements were taken on the exact same portion of the sample that had been exposed to narrow-band irradiation.

**Acknowledgments**—This work is part of a project No 2 219-0.84 of the "Schweizerischer Nationalfonds zur Förderung der Wissenschaftlichen Forschung". We would like to thank Mrs C. Monney for her help in the synthesis of the OTE precursors.

## REFERENCES

- T. Bally, S. Nitsche, K. Roth and E. Haselbach, *J. Am. Chem. Soc.* **106**, 3927 (1984).
- I. R. Dunkin, L. Andrews, J. T. Lurito and B. Kelsall, *J. Phys. Chem.* **89**, 1701 (1985).
- T. Bally, S. Nitsche, K. Roth and E. Haselbach, *J. Phys. Chem.* **89**, 2528 (1985); \*S. Nitsche, Dissertation, University of Fribourg (1985).
- B. J. Kelsall and L. Andrews, *J. Phys. Chem.* **88**, 2723 (1984).
- T. Bally, D. Hasselmann and K. Loosen, *Helv. Chim. Acta* **68**, 345 (1985).
- T. Shida, T. Kato and Y. Nosaka, *J. Phys. Chem.* **81**, 1095 (1977).
- E. Haselbach, T. Bally, R. Gschwind, U. Klemm and Z. Lanyiova, *Chimia* **33**, 405 (1979); \*T. Shida, E. Haselbach and T. Bally, *Accs. Chem. Res.* **17**, 180 (1984); \*E. Haselbach and T. Bally, *Pure Appl. Chem.* **56**, 1203 (1984).
- T. Shida, personal communication.
- H. D. Roth, *Proc. 10th IUPAC Symp. Photochem.*, p. 455f (1984); for a recent example, see: H. D. Roth and M. L. M. Schilling, *J. Am. Chem. Soc.* **107**, 716 (1985).
- V. Bondybej, *Adv. Chem. Phys.* **47**, 521 (1982).
- T. Shida, T. Momose and N. Ono, *J. Phys. Chem.* **89**, 815 (1985); L. Andrews, I. R. Dunkin, B. J. Kelsall and J. T. Lurito, *Ibid.* **89**, 821 (1985).
- L. Andrews, F. T. Prochaska and B. S. Ault, *J. Am. Chem. Soc.* **101**, 9 (1979).
- P. Datta, T. D. Goldfarb and R. S. Boiken, *J. Am. Chem. Soc.* **91**, 5429 (1969).
- W. R. Roth and B. Peltzer, *Chem. Ber.* **685**, 56 (1965).
- T. Bally, S. Nitsche and K. Roth, manuscript in preparation.
- S. W. Benson, *Thermochemical Kinetics*, 2nd Edn. Wiley, New York (1976).
- T. B. Jones and J. P. Maier, *Int. J. Mass Spectrosc. Ion Phys.* **31**, 287 (1979).
- R. B. Turner, B. J. Mallon, M. Tichy, W. v. E. Doering, W. R. Roth and G. Schroeder, *J. Am. Chem. Soc.* **95**, 8605 (1973).
- J. B. Pedley and J. Rylance, *Sussex-N.P.L. Computer Analyzed Thermochemical Data: Organic and Organometallic Compounds*, University of Sussex (1977).
- C. Batich, P. Bischof and E. Heilbronner, *J. El. Spectrosc. Rel. Phen.* **1**, 333 (1972).
- J. M. Greathead and S. W. Orchard, *Int. J. Chem. Kinet.* **15**, 1069 (1983).
- R. B. Turner, P. Goebel, B. J. Mallon, W. v. E. Doering, J. F. Coburn and M. Pomerantz, *J. Am. Chem. Soc.* **90**, 4315 (1968).
- R. Gleiter, K. Gubernator and W. Grimme, *J. Org. Chem.* **46**, 1247 (1981).
- R. B. Turner, W. R. Meadow and R. E. Winkler, *J. Am. Chem. Soc.* **79**, 4116 (1957).
- P. Bischof, J. A. Hashmall, E. Heilbronner and V. Hornung, *Helv. Chim. Acta* **52**, 173 (1969).
- K. Kimura, S. Matsumata, Y. Achiba, T. Yamazaki and S. Iwata, *Handbook of Hel Photoelectron Spectra of Fundamental Organic Compounds*. Japan Scientific Societies Press, Tokyo (1981).

- <sup>27</sup> T. Bally, R. Straub and K. Roth, *J. Am. Chem. Soc.*, submitted for publication.
- <sup>28</sup> T. Bally, S. Nitsche and K. Roth, *J. Chem. Phys.* **84**, 2577 (1986).
- <sup>29</sup> I. R. Dunkin and L. Andrews, *Tetrahedron* **41**, 145 (1986); see also E. Haselbach, T. Bally and Z. Lanyiova, *Helv. Chim. Acta* **62**, 577 (1979).
- <sup>30</sup> From the Raman spectrum, see: E. R. Lippincott, W. R. Fearheller and C. E. White, *J. Am. Chem. Soc.* **81**, 1316 (1959). From emission in n-alkane matrices, see: B. E. Kohler and J. B. Snow, *J. Chem. Phys.* **79**, 2134 (1983). From emission in a free jet, see: L. A. Heimbrook, B. E. Kohler and I. J. Levy, *Ibid.* **81**, 1592 (1984).
- <sup>31</sup> M. F. Granville, B. E. Kohler and J. B. Snow, *J. Chem. Phys.* **75**, 3765 (1981); L. A. Heimbrook, J. E. Kenny, B. E. Kohler and G. W. Scott, *Ibid.* **75**, 4338 (1981); B. E. Kohler, T. A. Spiglanin, J. R. Hemlin and M. Karplus, *Ibid.* **80**, 23 (1984).
- <sup>32</sup> M. F. Granville, G. R. Holtom and B. E. Kohler, *J. Chem. Phys.* **72**, 4671 (1980); B. E. Kohler and J. B. Snow *Ibid.* **79**, 2134 (1983).
- <sup>33</sup> A. C. Lasaga, R. J. Aerni and M. Karplus, *J. Chem. Phys.* **73**, 5230 (1980).
- <sup>34</sup> R. M. Gavin, C. Weisman, J. K. McVey and S. A. Rice, *J. Chem. Phys.* **78**, 522 (1978).